Comparative Study of Benzene···X (X = O_2, N_2, CO) Complexes Using Density Functional Theory: The Importance of an Accurate Exchange−Correlation Energy Density at High Reduced Density Gradients

T. A. Wesolowski,*† O. Parisel,† Y. Ellinger,‡ and J. Weber†

Département de Chimie Physique, Université de Genève, 30 quai Ernest-Ansermet, CH-1211 Genève 4, Switzerland, and Laboratoire d'Etude Théorique des Milieux Extrêmes, Ecole Normale Supérieure, 24 rue Lhomond, F-75231 Paris Cedex 05, France

Received: February 17, 1997; In Final Form: July 18, 1997[⊗]

Although density functional theory (DFT) is more and more commonly used as a very efficient tool for the study of molecules and bulk materials, its applications to weakly bonded systems remain rather sparse in the literature, except studies that consider hydrogen bonding. It is, however, of essential interest to be able to correctly describe weaker van der Waals complexes. This prompted us to investigate more precisely the reliability of several widely-used functionals. The equilibrium geometries and the binding energies of C_6H_6···X (X = O_2, N_2, or CO) complexes are determined within the standard Kohn−Sham approach of DFT using different exchange−correlation functionals and at the MP2 level of theory for comparison. It is comprehensively concluded that extreme care must be taken in the choice of the functional since only those that behave properly at large and intermediate values of the reduced density gradient s give relevant results. The PW91 exchange functional, the enhancement factor of which does not diverge at increasing *s*, appears as the most reliable for the studied systems. It is furthermore demonstrated that the quality of the DFT results is determined by the exchange energy component of the total energy functional.

1. Introduction

The gas/surface interaction chemistry, although having been studied for many years, both theoretically and experimentally, has recently been given a renewed interest as a consequence of the need for a proper modelization of dust and aerosol chemistry. It is now well-established, for example, that chemistry in the interstellar medium (ISM) should not be limited to gas-phase reactivity but must consider reactions at surfaces (silicates, ices, and crystalline or amorphous carbon): H_2, the most abundant molecular component in the universe, cannot be formed otherwise. Similarly, soots and residues of incomplete combustion of the biomass create solid particles which may dramatically modify the atmospheric chemistry. Among the possible surfaces available, graphite seems to be among the most effective both in the production of H_2 in noticeable proportions[1] and in the depletion of transition metals,[2] for example. It is thus of interest to consider the interaction of small molecules with graphite. Unfortunately, very little is known in this domain. In fact, some experimental results have been obtained from complexes of O_2, N_2, and CO with benzene, the basic constituent of graphite.[3−9] The above complexes, being much simplified models of the complexes formed in the ISM, provide a series of test cases for quantum chemistry calculations, making it possible to assess the quality of the applied theoretical approaches.

To some extent, the size of the model surface that should be finally considered in the calculation (at least a pyrene molecule if dealing with pregraphitic surfaces) precludes the use of common correlated ab initio approaches, such as MP2, due to the computational effort required. Semiempirical or molecular mechanics modelings would be attractive but have the drawback that their parameterization, which is based on well-behaving closed shell species, might lead to erroneous conclusions regarding the structure and the stability of the reactive species which are of interest in this type of chemistry. Following the previous outlines, density functional theory (DFT) calculations following the Kohn−Sham (KS) formalism appear as an alternative to ab initio or semiempirical calculations: no specific parameters are needed, and the intrinsic inclusion of correlation effects makes the results comparable to those obtained at least at the MP2 level of theory.

In this report, a first series of results is presented with the purpose to determine which functionals have to be used to properly describe the weak van der Waals molecular complexes that are expected upon the complexation of small diatomics onto a benzene molecule. The C_6H_6−X complexes are considered, where X stands for either O_2 ($X^3\Sigma_g^-$), N_2 ($X^1\Sigma_g^+$), or CO ($X^1\Sigma^+$): the results are compared to MP2 calculations and to the experimental data when available.

The MP2 level of theory is nowadays usually accepted as a good starting point to account for the correlation effects required to describe van der Waals systems: both subjects are reviewed in refs 10−13 and will not be detailed here. We only mention that the MP2 approach includes both intracorrelation, which results in having partially correlated interacting fragments, and some intercorrelation between the uncorrelated fragments, which recovers a large fraction of the dispersion energy.[14] Moreover, this approach is known to provide a wave function leading to fair multipole moments.[15] It is thus attractive to compare the MP2 and KS results for a variety of functionals keeping in mind that DFT methods are still not generally accepted as reliable modeling techniques for studying weak van der Waals complexes. Despite their remarkable successes in the studies of solid structures, as well as covalent or ionic systems, only a small fraction of DFT studies reported in the literature deals with such complexes.[16−23] This might be due to the fact that the term "DFT methodology" covers a whole range of approximations and simplifications; moreover, each particular implementation may lead to somewhat different results. The

† Université de Genève.
‡ Ecole Normale Supérieure.
[⊗] Abstract published in *Advance ACS Abstracts,* September 15, 1997.

S1089-5639(97)00586-0 CCC: $14.00

present paper attempts thus to rationalize some of the differences among DFT results.

The most fundamental differences between various DFT schemes arise from the unknown character of the exact analytic form of the exchange−correlation functional, $E_{xc}[\rho]$, involved in the Kohn−Sham formalism. Different DFT methods use different approximate functionals which are obtained using different strategies and which satisfy the scaling and asymptotic properties of the exact functional to a varying degree.[24−26] The hybrid methods, in which the approximate exchange−correlation functional is derived making use of the exact expression of the exchange energy applied to Kohn−Sham orbitals, were shown to be not applicable for studying the energetics of several complexes of the London type:[17,23] the interaction energies obtained this way are not attractive enough. Therefore, the hybrid functionals will not be considered here. The functionals credited with much success in molecular and atomic studies derive from the generalized gradient approximation (GGA)[27] where the local density approximation (LDA)[28] analytical form of $E_x[\rho]$ and $E_c[\rho]$ has been extended to include the density gradient dependency. Although being approximate, gradient-dependent $E_x[\rho]$ and $E_c[\rho]$ functionals usually lead to much better results than those obtained within the LDA scheme. Still, even if only gradient-dependent functionals are considered, the interaction energies differ between each other by about 1−2 kcal/mol for hydrogen-bonded systems (see ref 18, for instance).

The dispersion interactions have been recognized for their difficulty in accounting for by means of standard approximate exchange−correlation functionals within the Kohn−Sham framework.[19−23] One of the ways to overcome this difficulty is to use semiempirical corrections (see for example ref 23). It should be kept in mind that dispersion effects would be exactly accounted for if the exact exchange−correlation functional were known. Usually, the approximate exchange−correlation functionals are expressed as a sum of its exchange (E_x) and correlation (E_c) components. The distinction is rather arbitrary and does not correspond to the definition of exchange and correlation energies as defined in traditional ab initio methods. From the purely numerical point of view, the exchange energy functional represents the dominant part of the exchange−correlation functional. Its accuracy is, therefore, a dominant factor determining the quality of Kohn−Sham results. In particular, the choice of the correlation part of the approximate exchange−correlation functional does not significantly affect the Kohn−Sham results obtained with the same exchange functional for van der Waals complexes.[17,20]

The reasons for the discrepancies among the interaction energies derived from DFT calculations may be found through the inspection of the analytic form of the approximate functionals at large values of the reduced density gradient:

$$s = \frac{|\nabla\rho|}{2\rho\mathbf{k}_f} \tag{1}$$

where ρ is the density, and $\mathbf{k}_f$ is the local Fermi vector defined as

$$\mathbf{k}_f = (3\pi^2\rho)^{1/3} \tag{2}$$

Dealing with the exchange functional, one has, for instance,

$$E_x[\rho] = C_x\int \rho^{4/3}F_x(s)\, d^3r \tag{3}$$

where $F_x(s)$ denotes the enhancement factor, and where $C_x = (3/(4\pi))^{1/3}$. Most of the currently used gradient-dependent exchange energy functionals have their analytical form as in eq 3: the gradient dependency of the exchange energy density is contained in the F_x factor.

In the weak van der Waals complexes at their equilibrium geometry, the density overlap is usually small whereas the s values calculated for the electronic densities of the individual molecules forming the complex are large.[29] Consequently, one can expect that the exchange and correlation energy contributions to the interaction energy *strongly* depend on the behavior of the exchange−correlation energy density at large s. In the present study, several functionals are considered that differ in the analytical form of their enhancement factors $F_x(s)$. Included are functionals that range from the one of Perdew and Wang (PW91)[30] where $F_x(s)$ approaches 0 for large s to the one of Becke (B88)[31] where $F_x(s)$ tends to infinity with increasing s.

2. Methodologies and Computational Details

MP2 calculations were performed using the Gaussian-94 package.[32] In order to avoid artifacts due to the core correlation intrinsically accounted for in DFT calculations, all electrons were active in the perturbation. The 6-31G** basis set[33] was used. The potential energy curves obtained from these MP2 calculations stand as a reference for the discussion of several approximations pertinent to the Kohn−Sham formalism.

In an attempt to assess the reliability of the MP2 results, additional calculations were made at selected geometries of the investigated complexes using correlation treatments at higher levels: MP3, MP4(SDTQ), and coupled-cluster (including singles and doubles, namely CCSD, and even the correction for triples, CCSD-T). These calculations were performed at the geometry obtained at the MP2 level corrected for basis set superposition error. Since we expect core correlation and core−valence correlation effects not to be essential in the phenomena investigated, core orbitals were frozen, in these refined approaches, to retain tractable computational times.

All DFT calculations were performed applying the Kohn−Sham (KS) formalism.[34] The standard program deMon/KS[35] was used. The LDA results were obtained with the exchange energy given by the Dirac expression[36] and by the Vosko−Wilk−Nursair expression for the correlation energy.[28] The following acronyms for gradient-dependent functionals will be used in the text: PW86/P86, $E_x[\rho]$ taken from ref 27 and $E_c[\rho]$ from ref 37; B88/P86, $E_x[\rho]$ taken from ref 31 and $E_c[\rho]$ from ref 37; and PW91: $E_x[\rho]$ and $E_c[\rho]$ taken from ref 30.

In the DFT calculations, Gaussian basis sets were used to expand one-electron orbitals and to fit, by means of auxiliary functions, the electrostatic and the exchange−correlation potentials. The atomic orbitals were constructed from the following contraction patterns: (5211/411/1) for carbon, nitrogen, and oxygen, and (41/1) for hydrogen.[38] This basis set is comparable to the 6-31G** one, which is standard in quantum chemistry. The coefficients of the auxiliary functions were taken from ref 38: (5,2;5,2) for carbon, nitrogen, and oxygen, and (5,1;5,1) for hydrogen atoms. This orbital basis set together with the associated auxiliary functions will hereafter be referred to as basis I. In order to investigate the influence of the basis set expansion on the DFT results, some calculations were made using another basis set (basis II).[16] Basis II corresponds to the (7111/411/1*) contraction pattern associated with the (4,4;4,4) auxiliary functions for C, N, and O and is combined with the previous basis set for hydrogen.

The grids considered for the computations comprised 64 radial shells for the LDA and B88/P86 functionals, differing from the PW86/P86 and the PW91 functionals for which 128 radial shells were used. At the end of the self-consistent field (SCF)

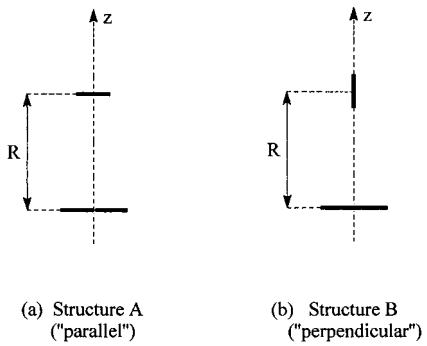

Figure 1. Structures of the studied molecular complexes: (a) parallel arrangement (C_{2v} symmetry) and (b) perpendicular arrangement (C_{6v} symmetry). In both cases, R stands for the distance between the benzene plane and the center of the diatomic bond.

procedure, each radial shell had either 50, 110, or 194 angular points (this corresponds to the "FINE" grid in the program deMon).

The basis set superposition error (BSSE) on the DFT and MP2 interaction energies was estimated according to the counterpoise method,[11,39] which was applied to each point of the energy curve.

Two geometrical arrangements of the complexes were considered: the first one (A, Figure 1a) has a C_{2v} (or C_s) symmetry, whereas the other one (B, Figure 1b) corresponds to a C_{6v} structure. Structures A and B will sometimes be referred to as "parallel" and "perpendicular" arrangements, respectively. All interaction energy curves correspond to rigid geometries of the interacting molecules: $R_{CC} = 1.42$ Å and $R_{CH} = 1.10$ Å for benzene; $R_{OO} = 1.21$ Å, $R_{NN} = 1.098$ Å, and $R_{CO} = 1.128$ Å for the diatomics under investigation.

The characteristics of the potential energy curves, i.e. the position of the minimum (R_0), the binding energy (E_{int}), and the second derivative of the energy with respect to the intermolecular distance were obtained by fitting third-order polynomials to 7−9 points. The second derivatives were used to derive the frequencies of the intermolecular stretching vibration by means of the one-dimensional oscillator model.

3. Results

3.1. The $C_6H_6\cdots O_2$ Complex. The interaction energy was calculated for several distances (R) between the benzene ring and the O_2 molecule. The potential energy curves obtained using MP2 and different DFT methods (basis I) are presented in Figure 2a for structure A of the complex. The minimum energy parameters are collected in Table 1 for both structures.

At the MP2 level of calculations, our BSSE-corrected structures and binding energies are in rough agreement with those reported by Granucci and Persico[40] for both structures A and B: our computed equilibrium distances appear to be larger by about 0.2 Å for structure A (0.1 Å for structure B), whereas the interaction energies are too small by 0.7 kcal/mol for structure A (0.5 kcal/mol for structure B). It follows that our results compare less favorably with the available experimental data, although the agreement still remains fair. The comparisons between obtained theoretical results and experimental results available for this system can hardly be conclusive. The experimental geometry is not known, and the binding energy is not directly observed. The error bars on experimental dissociation enthalpy[3,4] and free energy of dissociation fall in the range of 0.3 kcal/mol. The experimental errors are even larger than zero-point vibration energies (amounting to about 0.2 kcal/mol[40]) associated with intermolecular motions. The calculated potential energy curves are not symmetric. Due to

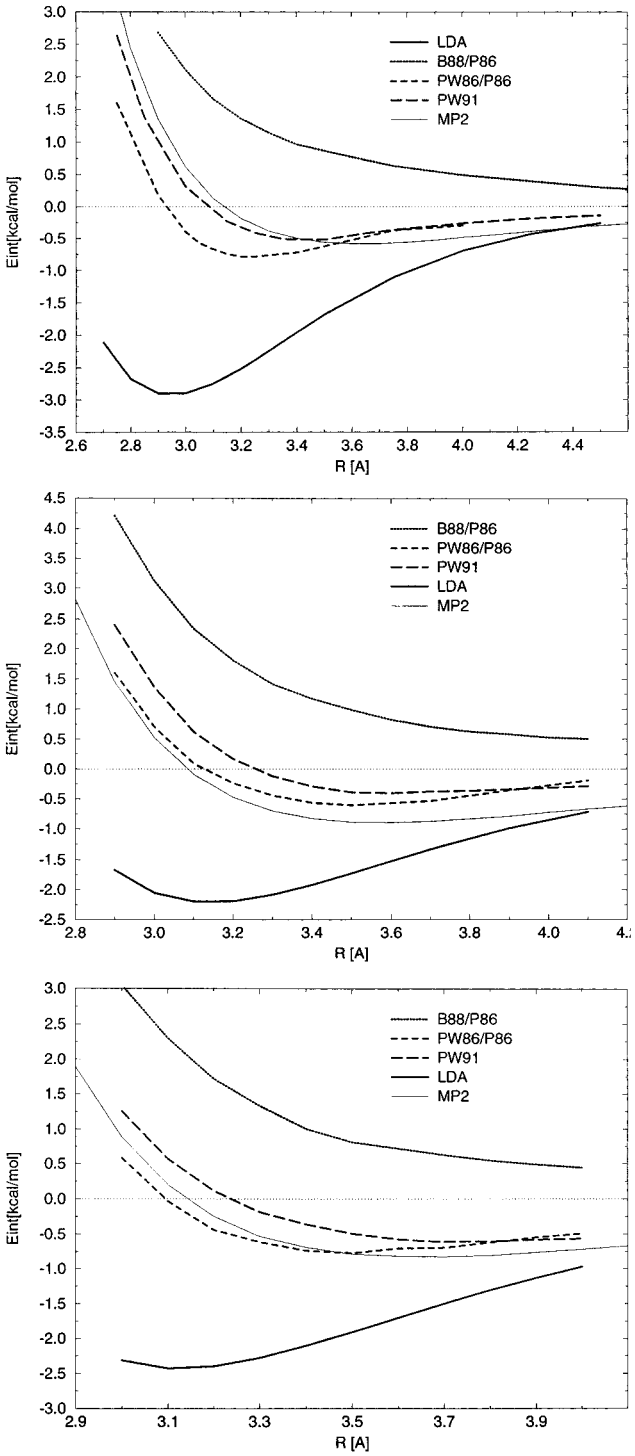

Figure 2. BSSE-corrected interaction energy curves for the $C_6H_6\cdots X$ complexes in their parallel arrangements (structure A): (a) $X = O_2$, (b) $X = N_2$, and (c) $X = CO$.

the asymmetry, the mean intermolecular distance is larger than the distance corresponding to the minimum of the curve. The shift is, however, not significant: it amounts to less than 0.05 Å for the zeroth oscillatory level that lies only 0.15 kcal/mol above the minimum of the curve.

The difference between our calculations and the MP2 calculations reported in ref 40 results certainly from the choice of the basis set. In the present case, standard polarization functions were used, which are known to underestimate dipole polarizabilities, whereas optimized polarization functions designed to properly account for dispersion interactions were used in ref 40.

TABLE 1: Equilibrium Intermolecular Distance (Å) and Binding Energy (kcal/mol) of the $C_6H_6\cdots O_2$ Complex at the MP2 and Different DFT Levels of Calculation

	structure A		structure B	
method	R_0	E_{int}	R_0	E_{int}
MP2[a]	3.21	1.52	3.71	1.18
MP2(BSSE)[a]	3.55	0.56	4.01	0.42
MP2(BSSE)[b]	3.36	1.24	3.9	0.87
KS/LDA	2.91	4.49	3.29	3.73
KS/LDA(BSSE)	2.95	2.93	3.34	2.11
KS/B88/P86	3.86	0.34	≥ 4.2[f]	≥ 0.38
KS/B88/P86(BSSE)[c]				
KS/PW86/P86	3.17	2.12	3.68	1.65
KS/PW86/P86(BSSE)	3.22	0.79	3.80	0.37
KS/PW91	3.36	1.65	3.71	1.20
KS/PW91(BSSE)	3.44	0.53	4.47	0.47
KS/PW91[g]	3.39	1.31	3.91	0.77
KS/PW91(BSSE)[g]	3.69	0.67	4.12	0.51
expt[d]		$\Delta G_{295\ K} = 1.2 \pm 0.3$		
exptl[e]		$D_2 = 1.65 \pm 0.32$		

[a] This work. [b] Reference 40. [c] No minimum was found at this level of calculation. [d] Reference 3: the structure is not experimentally determined. [e] Reference 4: the structure is not experimentally determined. [f] Approximate estimation owing to the divergence of the SCF procedure for distances larger than the quoted value. [g] Basis II.

Turning to DFT calculations, it clearly appears that the B88/B86 functional overestimates the intermolecular repulsion. After introduction of the BSSE corrections, the minimum that was initially present on the uncorrected curve even disappears! On the other hand, the LDA functional leads to a too strong intermolecular attraction. A similar overestimation of intermolecular energies, which results in the shortening of the equilibrium distance, was reported previously for other van der Waals complexes.[16,18]

The KS(PW86/P86) and KS(PW91) results are similar to each other and to the MP2 ones. The interaction energy curve which is the most similar to the MP2 one is obtained using the PW91 functional: this applies for both the BSSE-corrected and uncorrected interaction energies. For instance, the BSSE-corrected KS(PW91) methodology leads to an equilibrium intermolecular distance which is 0.11 Å shorter than the corresponding distance derived from the BSSE-corrected MP2 calculations, whereas using KS(PW86/86) leads to a larger difference: the discrepancy is now as high as 0.33 Å (structure A, basis I). Moreover, the binding energy obtained at the BSSE-corrected KS(PW91) level of theory differs by only 0.03 kcal/mol from the MP2 one, while the same quantity becomes as large as 0.23 kcal/mol using the KS(PW86/P86) values. The same trends are observed for structure B, with the noticeable exception that the MP2(BSSE) and the KS/PW91(BSSE) results are in excellent agreement provided that basis II is used.

The BSSE magnitude is similar for both MP2 and KS energies. At the equilibrium geometry, it equals 0.97 kcal/mol for MP2 and 1.5, 1.3, and 1.0 kcal/mol for KS(LDA), KS(PW86/P86), and KS(PW91), respectively, for basis I. The similarity between the BSSE effects in the MP2 and in the KS calculations using comparable basis sets was also reported previously[17] for weak van der Waals complexes. The KS(PW91) calculations show that the BSSE is reduced almost twice if basis II is used, which leads to a slight increase of the binding energy.

The MP2 and KS(PW91) interaction energy curves were used to derive the frequency of the vibration corresponding to the vertical intermolecular stretching mode for both the parallel and the perpendicular arrangements. At the parallel structure, the KS(PW91) and MP2 frequencies amount to 54.9 and 60.5 cm^{-1}, respectively. At the perpendicular orientation, the corresponding frequencies are 32.0 and 49.1 cm^{-1}. The frequencies obtained by means of both methods agree reasonably. The experimental frequencies of the considered stretching mode are not available. For the parallel structure, Granucci and Persico[40] derived the frequency of the intermolecular stretching mode (55 cm^{-1}) from their MP2 calculations which is in remarkable agreement with our values.

TABLE 2: Equilibrium Intermolecular Distance (Å) and Binding Energy (kcal/mol) of the $C_6H_6\cdots N_2$ Complex at the MP2 and Different DFT Levels of Calculation

	structure A		structure B	
method	R_0	E_{int}	R_0	E_{int}
MP2[a]	3.25	2.1	3.71	0.97
MP2(BSSE)[a]	3.60	0.85	4.16	0.13
MP2(BSSE)[b]	3.46	1.70	3.8	0.85
KS/LDA	3.10	3.74	3.35	3.71
KS/LDA(BSSE)	3.15	2.22	3.40	2.09
KS/B88/P86	3.87	0.48		
KS/B88/P86(BSSE)[c]				
KS/PW86/P86	3.41	1.93	3.78	1.75
KS/PW86/P86(BSSE)	3.53	0.60	3.93	0.30
KS/PW91	3.51	1.43	4.15	1.17
KS/PW91(BSSE)	3.59	0.40	4.66	0.32
KS/PW91[g]	3.56	1.40	4.10	0.51
KS/PW91(BSSE)[g]	3.83	0.74	4.34	0.28
exptl[d]	3.5			
exptl[e]	3.3	1.43		
exptl[f]		$D_e = 0.92 \pm 0.07$		

[a] This work. [b] References 12, 41. [c] No minimum was found at this level of calculation. [d] References 6, 8. [e] Reference 5. [f] Reference 7. [g] Basis II.

Finally, all MP2, KS(PW91), and KS(PW86/P86) calculations indicate that structure A (Figure 1), which exhibits interacting molecules in a parallel arrangement, is more stable than structure B where the mutual orientation is perpendicular (Table 1). This is in accordance with other works[4,40] that have further shown that the rotation of the diatomic around the C_6 symmetry axis of the benzene molecule is almost free.

3.2. The $C_6H_6\cdots N_2$ Complex. The potential energy curves for structure A (Figure 1) were calculated using basis I and the LDA, B88/P86, PW91, and PW86/P86 functionals. The equilibrium parameters are summarized in Table 2.

Our BSSE-corrected MP2 binding energy falls in the experimental range, differing from the theoretical results reported in refs 12 and 41: the equilibrium geometry differs only by 0.1 Å from the experimental values. Experimental investigations based on the analysis of the rotational spectrum[6,8] all indicate that the complex is a symmetric top, which is confirmed by our calculations. The parallel structure is the most stable, but due to the almost free rotation of N_2 around the benzene C_6 symmetry axis,[12,41] the sixfold-symmetry axis of C_6H_6 is preserved.

The KS(PW86/P86) and KS(PW91) results are similar to each other (Figure 2b, structure A) and to the MP2 ones. The B88/P86 exchange−correlation functional leads to a repulsive interaction curve for the geometry investigated, while LDA overestimates the binding energy, as is usually the case. The KS(PW91) and MP2 equilibrium intermolecular distances are almost identical (3.60 and 3.59 Å, respectively). The PW96/P86 functional leads to a shorter intermolecular distance (3.53 Å). On the other hand, the KS(PW86/P86) interaction energy (0.60 kcal/mol) differs less from the MP2 (0.86 kcal/mol) than that obtained from the KS(PW91) calculations (0.40 kcal/mol). The BSSE correction is similar for all methods. At the equilibrium geometry, it equals 1.5, 1.3, 1.2, and 1.0 kcal/mol, for KS(LDA), KS(PW86/P86), KS(PW91), and MP2 energies respectively. For the perpendicular arrangement, MP2, KS-(LDA), KS(PW86/P86), and KS(PW91) calculations were also made (see Table 2). The BSSE-corrected values of the

TABLE 3: Equilibrium Intermolecular Distance (Å) and Binding Energy (kcal/mol) Characteristics of the $C_6H_6\cdots CO$ Complex (Structures A, B1, and B2) at the MP2 and Different DFT Levels of Calculation

	structure A		structure B1		structure B2	
method	R_0	E_{int}	R_0	E_{int}	R_0	E_{int}
MP2	3.31	2.21	3.89	0.73	3.76	1.05
MP2(BSSE)	3.72	0.76	4.46	0.10	4.19	0.30
KS/LDA	3.09	3.53	3.53	2.94	3.40	2.64
KS/LDA(BSSE)	3.13	2.43	3.60	1.78	3.53	1.24
KS/B88/P86	4.05	0.27				
KS/B88/P86(BSSE)[a]						
KS/PW86/P86	3.44	1.67				
KS/PW86/P86(BSSE)	3.48	0.78				
KS/PW91	3.64	1.38	4.24	0.91	3.97	0.97
KS/PW91(BSSE)	3.71	0.61	4.39	0.22	4.47	0.29
KS/PW91[d]	3.70	1.10	4.38	0.17	4.18	0.27
KS/PW91(BSSE)[d]	3.90	0.70	4.51	−0.07	4.27	0.26
expt[b]	3.24	1.75				
expt[c]	3.44					

[a] No minimum was found at this level of calculation. [b] Reference 5. See text for details. [c] Reference 9. [d] Basis II.

interaction energy at the minimum amount to 0.13, 2.09, 0.30, and 0.32 kcal/mol for the MP2, KS(LDA), KS(PW86/P86), and KS(PW91) methods, respectively. The KS(PW91) calculations show that the BSSE is reduced almost twice if basis II is used, which leads to a better agreement of BSSE-corrected interaction energies with experiment.

The MP2 and KS(PW91) interaction energy curves were used to derive the frequency of the vibration corresponding to the vertical intermolecular stretching mode for both the parallel and the perpendicular arrangements. For the parallel structure, the KS(PW91) and MP2 frequencies amount to 65.7 and 60.4 cm^{-1}, respectively. At the perpendicular orientation, the corresponding frequencies are 35.1 and 50.2 cm^{-1}. The frequencies obtained by means of both methods agree reasonably. Experimental frequency of the intermolecular stretching mode at the parallel orientation amounts to about 60 cm^{-1},[5] in remarkable agreement with our results, although the KS(PW91) frequencies are systematically lower than the MP2 ones. As in the case of the $C_6H_6\cdots O_2$ complex, the mean intermolecular distance is not affected significantly by the deviations of the potential energy curve from the parabolic shape. All methods predict that the parallel arrangement is more stable.

3.3. The $C_6H_6\cdots CO$ Complex. The potential energy curves for structure A (Figure 1a) were calculated using basis I and the LDA, B88/P86, PW91, and PW86/P86 functionals (Figure 2c). The computed binding energies are collected in Table 3. The KS(PW91) and KS(LDA) calculations were also made for two orientations of the CO molecule in the perpendicular arrangement (structures B, Figure 1b): one (structure B1) where the C atom points toward the benzene ring and the other (structure B2) with the opposite orientation of the CO molecule.

As can be seen from Table 3, all calculations predict the parallel arrangement to be the most stable, in agreement with ref 5. At the MP2 level of calculation, the distance between the cycle and the diatomic is 3.31 Å, and the binding energy is 2.2 kcal/mol. Upon the BSSE correction, however, the equilibrium length is significantly increased by 0.4 Å while the stabilization energy is reduced to 0.76 kcal/mol. These results are nicely corroborated by the KS/PW91(BSSE) calculations (3.71 Å, 0.61 kcal/mol), whereas other functionals lead to uncomparable results. For both structures B1 and B2, a good agreement between the KS/PW91(BSSE) and MP2(BSSE) results is found provided basis II is used in the DFT calculations. The BSSE correction to the binding energy is observed to be almost the same using MP2 or KS/PW91 for B1 or B2. It is, however, larger at the MP2 level of calculation (1.45 vs 0.77 kcal/mol) for structure A. The KW(PW91) calculations show that the BSSE is reduced almost twice if basis II is used, which leads to a slight increase of the binding energy.

This complex was investigated experimentally by means of two-color time-of-flight mass spectroscopy.[5] The authors derived the structural and energetic properties not directly, but from the Lennard-Jones potential model, which was parametrized based on the observed spectroscopic properties. This model lead to the minimum energy structure which is similar to our structure A. The orientation of the interacting molecules is almost parallel (the angle between the benzene plane and the CO axis equals 75° with the oxygen atom pointing toward the aromatic ring), and the intermolecular distance amounts to 3.24 Å. The binding energy derived from this model amounts to 1.75 kcal/mol.

The MP2 and KS(PW91) interaction energy curves were used to derive the frequency of the vibration corresponding to the vertical intermolecular stretching mode for both the parallel and the perpendicular arrangements. At the parallel structure, the KS(PW91) and MP2 frequencies amount to 47.2 and 69.5 cm^{-1}, respectively. At the perpendicular orientation (B1), the corresponding frequencies amount to 19.9 and 36.6 cm^{-1} whereas, at the B2 orientation, they amount to 36.9 and 45.8 cm^{-1}, respectively. The frequencies obtained by means of both methods agree reasonably. Experimental frequency of the intermolecular stretching mode at parallel orientation amounts to about 66 cm^{-1},[5] in remarkable agreement with our results although the KS(PW91) frequencies are systematically lower than the MP2 ones, which agree better with the experimental values. As in the case of previously discussed complexes, the mean intermolecular distance is not affected significantly by the deviation of the potential energy curve from the parabolic shape.

4. Discussion

Basis set superposition error corrected binding energies of all considered complexes derived from the KS(PW91) and MP2 calculations are too low compared to experimental results. The differences are small compared to the differences between the energies derived from DFT calculations employing different approximations for the exchange−correlation functional. The theoretical determination of accurate structures and energies would require complete geometry optimizations, the obtainment of BSSE-free results, and the analysis of zero-point energy and anharmonicity effects. A full account of these effects is not possible for systems of the size of the complexes studied.

We must emphasize, however, that the aim of the present study is mainly the comparison of various approximations within the Kohn−Sham framework for a given level of basis set and not to derive highly accurate structures and energies for the species under investigation. Among the factors which might influence our analysis of the accuracy of the approximate exchange−correlation functionals, the most important ones are the effect of using incomplete basis sets on the MP2 and KS energies and the reliability of the second-order perturbation theory (MP2) to describe correlation effects. The effect of the basis set on the MP2 energies can be demonstrated by comparing our results with the ones taken from ref 40 which were obtained using larger basis sets. To minimize the importance of the basis set affects on our analysis of exchange−correlation functional approximations, similar basis sets of medium size were applied in both MP2 and KS calculations.

TABLE 4: MP2, MP3, MP4, and Coupled-Cluster Binding Energies (kcal/mol) for the $C_6H_6\cdots X$ Complexes Investigated[a]

	$C_6H_6\cdots O_2$		$C_6H_6\cdots N_2$		$C_6H_6\cdots CO$	
	no BSSE	BSSE	no BSSE	BSSE	no BSSE	BSSE
	Structure A		Structure A		Structure A	
MP2	1.52	0.56	2.1	0.85	2.21	0.76
MP3	0.93	0.17	1.14	0.32	1.21	0.46
MP4	1.30	0.36	1.60	0.61	1.44	0.69
	Structure B		Structure B		Structure B1	
MP2	1.18	0.42	0.97	0.13	0.73	0.10
MP3	0.60	0.07	0.39	0.20	0.28	−0.004
MP4	0.94	0.23	0.76	0.02	0.34	0.04
					Structure B2	
MP2					1.05	0.30
MP3					0.25	−0.10
MP4					0.54	0.15
CCSD					0.26	−0.10
CCSD-T					0.37	−0.02

[a] The geometries used correspond to the MP2 BSSE-corrected optimized geometries.

In an attempt to improve the calculated binding energies, and thus to assess the reliability of our MP2 results, we have refined the treatments of correlation effects through increasing the order of the perturbation: MP3 and MP4 calculations were made at the MP2(BSSE) optimized geometries. However, it can be seen from Table 4 that the perturbation series MP2, MP3, and MP4 does not lead to a monotonic convergence of the binding energies of the complexes studied, which is, unfortunately, the usual behavior of these approaches. For example, in the case of the $C_6H_6\cdots O_2$ complex, the binding energies obtained from single-point calculations at the MP3 level show significant discrepancies relative to the MP2 values. This applies for the parallel and the perpendicular structures and to both BSSE-corrected and not corrected binding energies. A binding energy of only 0.07 kcal/mol is obtained for structure B at the MP3-(BSSE) level, far from the MP2(BSSE) calculations (0.42 kcal/mol). For both orientations, the MP4 energies are in better agreement with the MP2 results than the MP3 calculations are; the MP4 approach, however, requires a much larger amount of central processing unit time. The results for the $C_6H_6\cdots CO$ complex provide another illustration of the nonmonotonic behavior of the perturbational series. The MP4(BSSE) energies are in good agreement with the MP2(BSSE) ones, especially for structures A and B1. For structures B1 and B2, MP3(BSSE) calculations indicate that the complex is not bounded, which led us to perform coupled-cluster calculations on structure B2. The obtained binding energies amount to 0.26 kcal/mol (CCSD) and 0.37 kcal/mol (CCSD-T), in agreement with the MP3 results. However, if the effect of the BSSE is included, the complex is not bounded: binding energies amount to −0.10 kcal/mol (CCSD) and −0.02 kcal/mol (CCSD-T), in line with the MP3 results (−0.10 /kcal/mol). Thus, in some cases, the agreement obtained between MP2, MP4, and MP3 energies is satisfactory, whereas the failure is dramatic in other cases: the discrepancies between the MP2 and MP3 binding energies can be as high as 1 kcal/mol (structure A of $C_6H_6\cdots N_2$). The agreement between MP2 and MP4 binding energies is, however, better since the discrepancies are lowered to 0.8 kcal/mol (no BSSE correction) and to 0.4 kcal/mol if the BSSE correction is made. The above results point out that increasing the order of the perturbation treatment will not necessarily and systematically result in having improved binding energies. Two reasons might be responsible for that. First of all, the MP*n* series is known to converge very slowly with increasing *n*.[42] The nonmonotonic character of this convergence further complicates any justification of the assessment that the results obtained at the order $n + 1$ will be better than the ones obtained at order *n*. Moreover, as observed by Frisch et al.,[43] the third- and fourth-order contributions to the binding energies may cancel each other *approximately*. In that case, the truncation of the perturbation series might take place at $n = 2$. This latter point is pointed out in ref 12 and discussed in ref 11 which summarizes the respective roles of the single, double, triple, and quadruple electronic excitations. Such a cancellation seems to occur in the present works and is reflected by the small variations (only a few tenths of a kcal/mol) in the binding energies, raising the correlation treatment from MP2 to MP4. Any detailed investigation on the convergence of the series would thus require MP*n* calculations with $n > 4$, which would involve a prohibitively large computational time owing to the size of the systems studied here.

The above observations on the variations of the binding energies when the level of correlation treatment is increased leads us to conclude that, although not necessarily fully converged to the limit, the MP2 binding energies provide a good estimate of the binding energies that could be obtained from more elaborated, and more costly, approaches.

The MP2 and the KS(PW91) calculations closely parallel one another if the characteristics of the potential energy curves at the minimum are analyzed. For all the conformations considered, the MP2 and the KS(PW91) interaction energies agree within 0.11 kcal/mol for O_2, 0.15 kcal/mol for N_2, and 0.06 kcal/mol for CO, provided basis II is used in the DFT calculations. We point out that the discrepancies observed between the MP2 and the KS(PW91) results are smaller than those observed between the MP2 and the MP3 or MP4 calculations. On the purely numerical point of view, this is the primary reason why the PW91 functional is, among the functionals considered here, the most attractive alternative to MP2 theory for studying not only the systems investigated in the present contribution, but their larger homologues. The agreement between our MP2 and KS(PW91) results should not be considered as fortuitous or as purely numerical: the better behavior of the PW91 functional, with respect to the other functionals considered here, relies on a physical basis as will be elaborated in the following.

In all molecular complexes studied, similar trends among results obtained using different functionals are observed. The LDA approximation leads to intermolecular distances that are too short and to interaction energies that are too strong. This tendency was reported for other complexes[16,18] and will not be discussed further here. Turning to gradient-dependent functionals, it appears that both PW86/P86 and PW91 lead to better interaction energy curves than B88/P86.

It is useful to recall that the PW86/P86 and the B88/P86 functionals share the same analytical form of the correlation energy. Consequently, the difference between KS(B88/P86) and KS(PW86/P86) results can be attributed solely to the difference in the corresponding exchange energy functionals which have the analytical form given in eq 3 and the following enhancement factors:

$$F_x^{PW86}(s) = (1 + \alpha s^2 + \beta s^4 + \gamma s^6)^{1/15} \qquad (4)$$

$$F_x^{B88}(s) = 1 + \frac{(gs)^2}{1 + \delta(gs)\sinh^{-1}(gs)} \qquad (5)$$

$$F_x^{PW91}(s) = \frac{1 + \zeta(gs)\sinh^{-1}(gs) + [\eta - \theta\exp(-100s^2)](gs)^2}{1 + \zeta(gs)\sinh^{-1}(gs) + 0.004s^4} \quad (6)$$

In these formulas, $\alpha-\zeta$ stand for adjustable parameters, $g = 2^{4/3}(3\pi^2)^{1/3}$, and s is the reduced density gradient defined in eq 1. In the $1.0 \le s \le 5.0$ range, the enhancement factor $F(s)$ of the B88 functional is larger than the corresponding factor of both the PW86 and PW91 functionals which have similar numerical values (Figure 3a).

The exchange energy contribution to the interaction energy, i.e.

$$\delta E_x = E_x(C_6H_6\cdots X) - E_x(C_6H_6) - E_x(X) \quad (7)$$

where X stands for either N_2, O_2, or CO, represents an integral of $F_x(s)$, weighted by a factor $\rho^{4/3}$ (eq 3), over regions with different s. Figure 4 shows the BSSE-corrected values of δE_x for several arrangements of the $C_6H_6\cdots O_2$ complex. The presented δE_x values were calculated using different approximate exchange functionals and corresponding electron densities.

The qualitative differences and similarities between interaction energies obtained with different approximate exchange−correlation functionals are reflected in δE_x. The δE_x^{PW91} and δE_x^{PW86} curves are almost parallel at intermediate intermolecular distances, which leads to similar positions of the corresponding interaction energy minima. The δE_x^{LDA} curve falls sharply with decreasing intermolecular distances, which results in the shift of the interaction energy minimum toward shorter intermolecular distances. The δE_x^{B88} values are least negative: this fact is related to the repulsive character of the corresponding interaction energy curve (Figure 2a).

An inspection of the s values for several intermolecular distances (Figure 3b) shows that, in the intermolecular region, the reduced density gradient increases with the intermolecular distance. This might result in a strong dependency of the exchange energy density upon the accuracy of the approximate exchange functional.

The known failure of the B88 exchange functional to describe correctly the van der Waals complexes reported by several investigators[17,19,20,22,23] originates from the fact that the B88 functional underestimates the intermolecular attraction due to the divergent behavior of its enhancement factor at large s. Despite the qualitatively different behavior of $F_x^{PW86}(s)$ and $F_x^{PW91}(s)$ at $s \ge 5.0$, and KS(PW86/P86) and KS(PW91) results are similar. This indicates that the regions characterized by this range of s contribute little to the exchange−correlation potential and energy due to the $\rho^{4/3}$ weighting factor.

The good agreement between the MP2 and the KS(PW91) potential energy surfaces originates from the fact that MP2 methods provide a fairly accurate scheme accounting for the correlation contributions whereas the PW91 functional provides, among the set of functionals used here, the most accurate approximation of the exact functional in the regions characterized by small electron density overlaps.

5. Conclusions

The results obtained for all van der Waals complexes studied here demonstrate that using the B88 functional for the exchange energy leads to qualitatively wrong results: only the PW86/P86 and PW91 exchange−correlation functionals lead to results comparable to the MP2 ones for a similar level of basis sets.

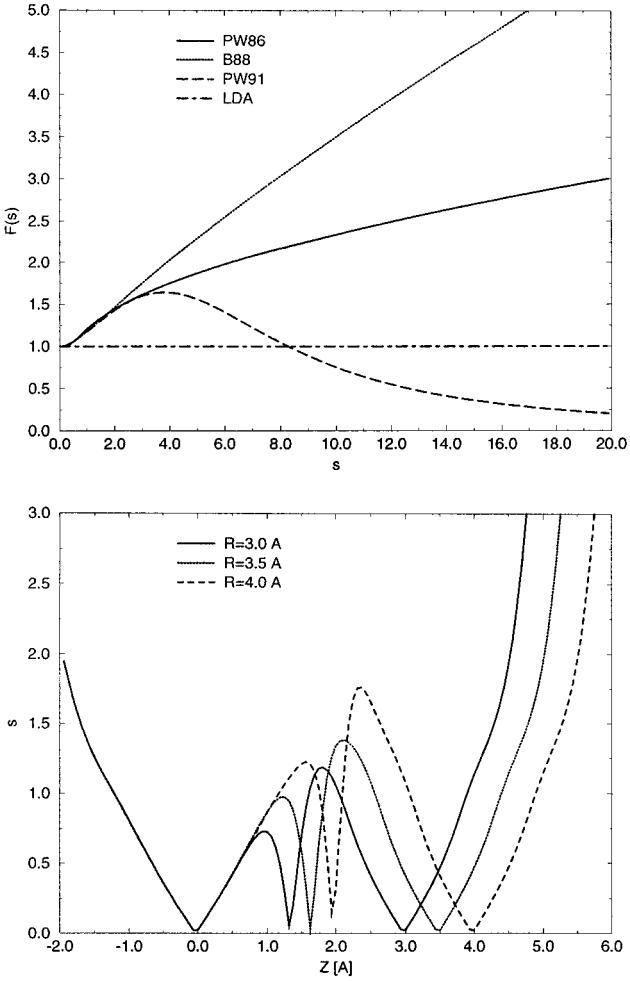

Figure 3. (a) The numerical value of the enhancement factor $F_x(s)$ for the exchange energy functionals described in text, and (b) the numerical value of the reduced density gradient s calculated along the C_2 symmetry axis for the $C_6H_6\cdots O_2$ complex at intermolecular distances equal 3.0, 3.5, and 4.0 Å.

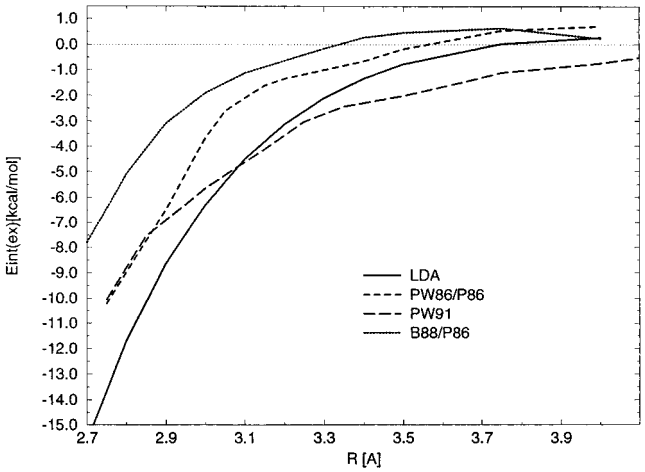

Figure 4. The exchange energy component of the interaction energy, $\delta E_x = E_x(C_6H_6\cdots O_2) - E_x(C_6H_6) - E_x(O_2)$, for structure A (parallel arrangement) of the $C_6H_6\cdots O_2$ complex.

We attribute the qualitative superiority of these two functionals to a better behavior of their corresponding enhancement factor F_x at intermediate reduced density gradients s; using F_x^{B88} results in an underestimated stabilizing exchange energy component of the total interaction energy. Finally, LDA leads to unrealistically strong interactions; consequently, the equilibrium distances are too short.

Although the PW86/P86 and PW91 results are usually similar, it is found that the potential energy curves obtained with the PW91 functional are closer to the MP2 ones than those obtained with the PW86/P86 functional. The KS(PW86/P86) calculations required paying more attention to the numerical integration than the ones using the PW91 functional. This is due to the divergent behavior of the corresponding enhancement factor at large s and small ρ. Therefore, although the KS(PW86/P86) results are only slightly inferior in quality than the KS(PW91) ones, we advocate selecting the PW91 functional for the study of similar van der Waals complexes.

Both the KS(PW91) and the MP2 methods lead to the same ordering of the minimum energy structure and predict parallel arrangements. The shortest intermolecular distance occurs in the $C_6H_6\cdots O_2$ complex (3.55 and 3.44 Å for MP2 and KS-(PW91), respectively) and the longest (3.72 and 3.71 Å, for MP2 and KS(PW91), respectively) occurs in the $C_6H_6\cdots CO$ complex. For all the conformations considered, the MP2 and KS(PW91) interaction energies agree within 0.11 kcal/mol for O_2, 0.15 kcal/mol for N_2, and 0.06 kcal/mol for CO, provided basis II is used in the DFT calculations. The PW91 functional, leading to the best agreement between the MP2 and the KS binding energies, also leads to frequencies agreeing within 17 cm^{-1} for the intermolecular stretching mode.

Finally, we would like to emphasize the importance of using well-behaving functionals regarding the exchange−correlation energy density at high reduced density gradient if aiming at studying weak van der Waals complexes with a large degree of confidence. In the presented studies the PW91 exchange functional is the only one with nondiverging $F(s)$ behavior at large s. Recently, other GGA functionals with similar properties were proposed.[44] According to our analysis, such functionals should lead to interaction energies which are less attractive than the ones derived by means of LDA and much better than the ones obtained using the B88 exchange functional. Indeed, Yang et al.[45] as well as Patton and Pederson[46] reported good results obtained for van der Waals complexes using such gradient-dependent functionals.

The present study shows that coupling the PW91 functional with the (7111/411/1*) basis set allows one to reproduce MP2 binding energies with confidence. This is thus a promising starting point in the quest for the methodologies required to study large weakly-bounded systems using a tractable basis set.

Acknowledgment. The authors are grateful to Prof. D. R. Salahub for providing a copy of the deMon program. The discussions with Prof. Weitao Yang are greatly acknowledged. Financial support by the Federal Office for Education and Science, acting as Swiss COST office, is greatly acknowledged. This work is also a part of the Project 20-41830.94 of the Swiss National Science Foundation. The authors are indebted to the Swiss Center for Scientific Computing (Manno, Switzerland) for supporting part of the calculations presented here. O.P. gratefully acknowledges the University of Geneva for a post-doctoral research fellowship.

References and Notes

(1) Barlow, M. J.; Silk, J. *Astrophys. J.* **1976**, *207*, 131.
(2) Marty, P.; Serra, G.; Chaudret, B.; Ristorcelli, I. *Astron. Astrophys.* **1994**, *282*, 916.
(3) Goodling, W. A.; Serak, K. R.; Ogilby, P. R. *J. Phys. Chem.* **1991**, *95*, 7868.
(4) Grover, J. R.; Hagenow, G.; Walters, E. A. *J. Chem. Phys.* **1992**, *97*, 628.
(5) Nowak, R.; Menapace, J. A.; Bernstein, E. R. *J. Chem. Phys.* **1988**, *89*, 1309.
(6) Weber, Th.; Smith, A. M.; Riedle, E.; Schlag, E. W. *Chem. Phys. Lett.* **1990**, *175*, 79.
(7) Ernstberger, B.; Krause, H.; Neusser, H. J.; *Z. Phys. D* **1991**, *20*, 189.
(8) Ohshima, Y.; Kohguchi, H.; Endo, Y. *Chem. Phys. Lett.* **1991**, *184*, 21.
(9) Brupbacher, Th.; Bauder, A. *J. Chem. Phys.* **1993**, *99*, 9394.
(10) van Lenthe, J. H.; van Duijnevelt−van de Rijdt, J. G. C. M.; van Duijnevelt, F. B. Weakly bonded systems. In *Ab initio Methods in Quantum Chemistry*; Lawley, K. P., Ed.; Wiley: New York, 1987; Vol. II.
(11) Hobza, P.; Zahradník, R. *Chem. Rev.* **1988**, *88*, 871.
(12) Hobza, P.; Selze, H. L.; Schlag, E. W. *Chem. Rev.* **1994**, *94*, 1767.
(13) Chalasiński, G.; Szcześniak, M. *Chem. Rev.* **1994**, *94*, 1723.
(14) Pople, J. A. *Faraday Discuss. Chem. Soc.* **1982**, *73*, 7.
(15) Diercksen, G. H. F.; Roos, B. O.; Sadlej, A. *Int. J. Quantum Chem.* **1983**, *517*, 265.
(16) Ruiz, E.; Salahub, D. R.; Vela, A. *J. Phys. Chem.* **1996**, *100*, 12265.
(17) Hobza, P.; Šponer, J.; Reschel, T. *J. Comput. Chem.* **1995**, *16*, 1315.
(18) Sule, P.; Nagy, A. *J. Chem. Phys.* **1996**, *104*, 8524.
(19) Perez-Jaroda, J. M.; Becke, A. D. *Chem. Phys. Lett.* **1995**, *233*, 134.
(20) Meijer, E. J.; Sprik, M. *J. Chem. Phys.* **1996**, *105*, 8684.
(21) Lundquist, B. I.; Andersson, Y.; Stiao, H.; Chan, S.; Langreth, D. C. *Int. J. Quantum Chem.* **1995**, *56*, 247.
(22) Kristyan, S.; Pulay, P. *Chem. Phys. Lett.* **1994**, *229*, 175.
(23) Šponer, J.; Leszczynski, J.; Hobza, P. *J. Comput. Chem.* **1996**, *17*, 841.
(24) Ernzerhof, M.; Perdew, J. P.; Burke, K. In *Density Functional Theory*; Nalewajski, R., Ed.; Springer: Berlin, 1996.
(25) Levy, M.; Perdew, J. P. *Int. J. Quantum Chem.* **1994**, *49*, 539.
(26) Neumann, R.; Nobes, R. H.; Handy, N. C. *Mol. Phys.* **1996**, *87*, 1.
(27) Perdew, J. P.; Wang, Y. *Phys. Rev. B* **1986**, *33*, 8800.
(28) Vosko, S. H.; Wilk, L.; Nursair, M. *Can. J. Phys.* **1980**, *58*, 1200.
(29) Wesolowski, T. A.; Chermette, H.; Weber, J. *J. Chem. Phys.* **1996**, *105*, 9182.
(30) Perdew, J. P.; Wang, Y. In *Electronic Structure of Solids' 91*; Ziesche, P., Eschrig, H., Eds.; Academie Verlag: Berlin, 1991; p 11.
(31) Becke, A. D. *Phys. Rev. A* **1988**, *38*, 3098.
(32) Frisch, M. J.; Trucks, G. W.; Schlegel, H. B.; Gill, P. M. W.; Johnson, B. G.; Robb, M. A.; Cheeseman, J. R.; Keith, T.; Petersson, G. A.; Montgomery, J. A.; Raghavachari, K.; Al-Laham, M. A.; Zakrzewski, V. G.; Ortiz, J. V.; Foresman, J. B.; Ciosloski, J.; Stefanov, B. B.; Nanayakkara, A.; Challacombe, M.; Peng, C. Y.; Ayala, P. Y.; Chen, W.; Wong, M. W.; Andres, J. L.; Replogle, E. S.; Gomperts, R.; Martin, R. L.; Fox, D. J.; Binkley, J. S.; Defrees, D. J.; Baker, J.; Stewart, J. P.; Head-Gordon, M.; Gonzalez, C.; Pople, J. A. *Gaussian-94, Revision B.1*; Gaussian, Inc.: Pittsburgh PA, 1995.
(33) Franckl, M. M.; Pietro, W. J.; Hehre, W. J.; BInkley, J. S.; Gordon, M. S.; DeFrees, D. J.; Pople, J. A. *J. Chem. Phys.* **1982**, *77*, 3654.
(34) Kohn, W.; Sham, L. J. *Phys. Rev.* **1965**, *140A*, 1133.
(35) St-Amant, A. Ph.D. Thesis, Université de Montréal, 1992.
(36) Slater, J. C. *Phys. Rev.* **1951**, *81*, 385.
(37) Perdew, J. P. *Phys. Rev. B* **1986**, *33*, 8822.
(38) (a) Sim, F.; Salahub, D. R.; Chin, S.; Dupuis, M. J. *J. Chem. Phys.* **1991**, *95*, 4317. (b) Sim, F.; St-Amant, A.; Papai, I.; Salahub, D. *J. Am. Chem. Soc.* **1992**, *114*, 4391.
(39) Boys, S. F.; Bernardi, F. *Mol. Phys.* **1970**, *19*, 553.
(40) Granucci, G.; Persico, M. *Chem. Phys. Lett.* **1993**, *205*, 331.
(41) Hobza, P.; Bludský, O.; Selzle, H. L.; Schlag, E. W. *J. Chem. Phys.* **1993**, *98*, 6223.
(42) Knowles, P. J.; Somasundram, K.; Handy, N. C.; Hirao, K. *Chem. Phys. Lett.* **1985**, *112*, 8.
(43) Frisch, M. J.; Pople, J. A.; Del Bene, J. E. *J. Phys. Chem.* **1985**, *89*, 3664.
(44) Perdew, J. P.; Burke, K.; Ernzerhof, M. *Phys. Rev. Lett.* **1996**, *77*, 3865.
(45) Zhang, Y.; Pan, W.; Yang, W. Presented at Symposium on Density Functional Theory and Applications, Duke University, Durham, NC, June 3−7, 1997.
(46) Patton, D. C.; Pederson, M. R. Presented at Symposium on Density Functional Theory and Applications, Duke University, Durham, NC, June 3−7, 1997.